Journal of Crystal Growth 87 (1988) 481–493
North-Holland, Amsterdam

GAS PHASE KINETICS ANALYSIS AND IMPLICATIONS FOR SILICON CARBIDE CHEMICAL VAPOR DEPOSITION

C.D. STINESPRING and J.C. WORMHOUDT

Center for Chemical and Environmental Physics, Aerodyne Research. Inc., 45 Manning Road, Billerica, Massachusetts 01821, USA

Received 15 September 1987

The purpose of this study was to evaluate the impact of gas phase chemistry on recently reported two step chemical vapor deposition processes for epitaxial β-SiC. Results are reported for equilibrium predictions of species concentrations near the substrate surface and kinetic calculations to determine if these equilibrium levels are obtained. These calculations indicate significant differences in the levels of hydrocarbon species as well as species containing silicon–carbon bonds for equilibrium versus kinetically limited situations. This result combined with available data on the surface chemistry of the affected species provides considerable insight into the deposition mechanism.

1. Introduction

Motivated by outstanding electrical and mechanical properties [1–3], chemical vapor deposition (CVD) of β-SiC is currently the subject of renewed interest. One of the major reported results has been the development of CVD processes capable of reproducibly growing high quality epitaxial thin films of β-SiC [4–7].

The deposition process originally described by Nishino and coworkers [4] involved two distinct steps: an initial growth period followed by a crystal growth period. During the initial growth period, the substrate was heated from room temperature to 1673 K in less than 60 s, maintained at this temperature for about 60 s, and then cooled to room temperature all while flowing 0.03 mol% C_3H_8 in H_2 over the substrate. This was followed by a crystal growth period during which the substrate was again rapidly heated to 1673 K in a flow of 0.02 mol% SiH_4 and 0.02 mol% C_3H_8 in H_2.

Subsequent modifications of the deposition process have simplified the procedure and involve introducing the SiH_4/C_3H_8 in H_2 gas mixture during the initial temperature ramp and eliminating the temperature cycling between the end of the initial growth and the beginning of the crystal growth periods [8]. Despite these changes, the technique should still be considered as a two step process since deposition during the temperature ramp is required to optimize the quality of the SiC produced during the subsequent constant temperature crystal growth period. A similar technique which uses C_2H_4 rather than C_3H_8 has been reported by Liaw and Davis [6]. They refer to growth during the initial temperature ramp as conversion of the Si surface.

The SiC layers formed during the temperature ramp or initial growth period mediate the transition from the underlying Si lattice to the epitaxial SiC deposit. According to Addamiano and Sprague [7], this deposit is 10 to 20 layers thick and is highly strained with a large number of internal surfaces. None of the studies performed to date, however, have provided a clear picture of the initial growth mechanism and how this mechanism relates to subsequent crystal growth. It is simply observed that omitting the initial growth step results in poor quality SiC. It is interesting to note that adding SiH_4 to the reactive gas mixture during the initial temperature ramp apparently does not alter the nature or function of the initially deposited layers.

0022-0248/88/$03.50

In this paper, we present a modeling analysis of gas phase chemical processes which occur during the initial and crystal growth periods. Results are reported for equilibrium predictions of species concentrations near the substrate surface and kinetic calculations to determine if these levels are attained. Based on these results, deposition species (i.e., species available for reaction on the heated substrate surface) for the initial and crystal growth periods are identified. The implications of our finding that the levels of some but not all deposition species are kinetically limited are discussed.

2. Method of analysis

Gas phase equilibrium calculations over the appropriate temperature range were used to identify the potentially important deposition species. Then, one-dimensional chemical kinetic calculations were performed along appropriate time–temperature profiles to study the evolution of the important gas phase species. In this section, the basic inputs to the modeling analyses are described. These are the time–temperature profiles and the thermodynamic and kinetics data bases.

2.1. Time–temperature profiles

The time–temperature profiles simulate the temperature changes experienced by reactive gas species as they diffuse to the surface and are approximations to a complete, coupled flow and kinetics model. In deriving profiles appropriate to the two-step CVD process, it is helpful to first consider the physical situation encountered in CVD processes. As illustrated in fig. 1, reactant gases enter the CVD reactor with a flow velocity, v_{F0}, and at essentially the same temperature as the upper cold wall ($T_C = 300$ K). As the gas passes over the hot substrate, T_H, temperature and concentration profiles are established in the boundary layer. Consequently, the gas is accelerated to a new flow velocity, v_F, and acquires a diffusional velocity, v_D, toward the substrate. The diffusion is driven by concentration gradients in the boundary layer and, when combined with the temperature gradient, imposes a "diffusional temperature ramp", $\dot{T}_D$, on the gas species as they diffuse to the substrate.

During the crystal growth period, $\dot{T}_D$ alone may be used to establish the time–temperature profile for gas species. The magnitude of $\dot{T}_D$ may be estimated using the equation

$$\dot{T}_D = v_D |\partial T/\partial Y|,$$

where $|\partial T/\partial Y|$ is the temperature gradient, and for a given gas phase species, v_D is defined by the equation

$$J = \rho v_D = \bar{\rho} D(\partial M/\partial Y),$$

where J is the flux, ρ is the mass density, and D is the diffusion coefficient for a given species. The quantity $\bar{\rho}$ is the mass density of the gas and $M = \rho/\bar{\rho}$ is the mass fraction of a given species.

During the initial growth regime, the situation is complicated by the fact that the substrate temperature is ramped to 1673 K at a rate, $\dot{T}_H$, of approximately 70 K s^{-1}. In this case, $\dot{T}_H$ or $\dot{T}_D$ may separately or in combination define the time–temperature profile for the gas phase reactants. To obtain additional insight on this point

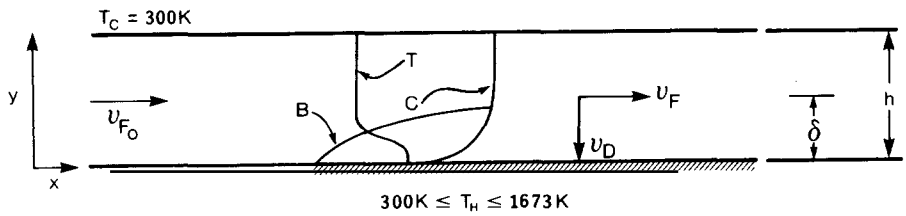

Fig. 1. Schematic representation of CVD reactor and process parameters. The boundary layer (B) and evolving temperature (T) and concentration (C) profiles are indicated as are the forced (v_F) and diffusional (v_D) flow velocities.

and to calculate the time–temperature profiles, specific assumptions about the temperature and concentration profiles must be made.

We assumed that the temperature profile was fully developed (i.e., linear) for each specific value of the substrate temperature, T_H, considered during the temperature ramp. Thus, $|\partial T/\partial Y| = (T_H - T_C)/h$. This approximation can be justified by considering some numerical estimates. The distance required to fully develop the temperature profile (the thermal entrance length) is given by [9] $l = 0.04\ h\ \mathrm{Re}$, where $\mathrm{Re} = v_F \rho h/\eta \propto T^{-1.7}$ is the Reynolds number. Here, η is the viscosity of the gas at temperature T. The time period required to fully developed the thermal boundary layer is

$$\tau = l/v_F = \tau_0 (T_0/T)^{2.7},$$

where τ_0 is the characteristic time at temperature T_0. For a H_2 carrier gas with $v_{F0} = 1$ cm s^{-1} and $h = 2.5$ cm, the time required to fully develop the thermal boundary layer is on the order of 0.2 s at 300 K and 2×10^{-1} s at 1673 K. From these values, it may be seen that the time required to fully develop the thermal boundary layer is quite short compared to the time in which the imposed temperature ramp changes T_H significantly. This is especially true at higher temperatures where significant gas phase chemistry is expected to occur.

Initially, a linear concentration profile over the boundary layer was considered. In this case, v_D was given by

$$v_D = \frac{D}{M}\frac{\partial M}{\partial Y} \sim \frac{2D}{\delta}.$$

Here δ is the thickness of the fully developed boundary layer. We assumed δ to be equal to $h/2$. Also, $D = D_0 (T/T_0)^{1.73}$ where we took D_0 as 0.37 cm^2 s^{-1} at 300 K for SiH_4 in H_2. For these values, we find $v_D \sim 12$ cm s^{-1}, $|\partial T/\partial Y| = 549.2$ K cm^{-1}, and $\dot{T}_D = 6590$ K s^{-1} for $T_H = 1673$ K and $h = 2.5$ cm. From this estimate it is clear that $\dot{T}_D \gg \dot{T}_H$, and in defining the time-temperature profile, the diffusional rather than the imposed substrate temperature ramp places the most severe demands on the chemical kinetics. That is, $\dot{T}_D$ rather than $\dot{T}_H$ is the temperature rate of change which should be used to initial crystal growth regimes.

As this study evolved, different concentration profiles were considered. The linear concentration profile overestimates $\dot{T}_D$ in the cooler regions and underestimates it in the hotter regions. To eliminate this difficulty, $\dot{T}_D$ was calculated using concentration profiles similar to that illustrated in fig. 1. These were determined using a diffusion code combined with a equilibrium chemistry code [10]. This results in a more accurate representation of the problem, and the calculations obtained using this approach will form the basis of our subsequent discussions. It should be noted, however, that our basic conclusions are the same for either choice of diffusion profiles.

2.2. Thermodynamic data base

The tables of reaction mechanisms given in appendix A serve to indicate to chemical species considered in this work. A number of a simpler molecules involved in the calculations are listed in the JANAF Thermochemical Tables [11]. Data for additional species were taken from Benson [12] and Stull et al. [13] up to the highest temperature listed and then extrapolated to 1800 K. For silicon species including SiH_2, SiH_3, and Si_2H_6, heat of formation values were taken from Walsh [14] with structures and vibrational frequencies obtained from spectroscopic observations. Recent matrix studies by Hauge and co-workers [15] had completely reassigned the SiH_2 band and also put the SiH_3 assignments in doubt. However, these new data still result in vibrational frequencies that are essentially equivalent for a purpose of calculating thermodynamic properties. On the other hand, replacing the 59.3 kcal/mol SiH_2 heat of formation used here with the 65 kcal/mol value recently recommended by Walsh [16] would result in SiH_2 concentrations at high temperatures about a factor of five lower than those reported here, Si_3 concentrations a factor of more than two higher, and small increases in other species. The 65 kcal/mol value is in turn lower than the 69 kcal/mol recently measured by Shin and Beauchamp [17] and the theoretical value of 68.1 kcal/mol reported by Ho et al. [18]. The latter paper, a useful source of

thermodynamic parameters for SiH_x species, appeared after our calculations were completed. A companion paper on Si_2H_x radicals by the same authors [19] was also not available at the time of the work reported here; thus, more approximate estimation methods were used. The conclusions presented here, however, are not altered by these new data.

In table 3, Si_2H_4 and SiH_3SiH refer to disilene and silylsilylene, respectively. The heat of formation for disilene is from Ring and co-workers [20], the structure is a theoretical prediction [21], and vibrational frequencies are estimated by scaling C_2H_4 values by the ratios of Si_2H_6 to C_2H_6 frequencies. We expected the heat of formation values of the two isomers to be within 10 kcal/mol of each other and so chose a value for silylsilylene based on the assumption that ΔH values for H_2 removal from it and silane are the same. Entropy and heat capacity values were assumed to be the same for both isomers. For Si_2H_x species where parameters were not available, the heat capacity and entropy values were estimated by analogy to carbon compounds, using scaling factors from known silicon parameters. For Si_2H_5, the heat of formation was taken from Walsh, while for the other species, the values estimated by Schmitt [22] were adopted. An alternate method for estimating these parameters by analogy to carbon compounds yields values similar to those calculated in ref. [19]. If those values were used, Si_2H_2 and Si_2H_4 rather than Si_2H and Si_2H_3, as reported here, would be the most important Si_2H_x species.

Information on larger compounds, although even sparser, was adequate for estimation as described above. Benson and co-workers [12] have considered a few silicon species including Si_3H_8. This estimate along with the JANAF Si_3 values form two extreme cases which can be compared with their carbon analogs, after which the relationships observed can be used to scale parameters for other C_3H_x species to yield values for Si_3H_x molecules. Similarly, both experimental [20] and calculated [23] heats of formation as well as entropy and heat capacity values based on a correlation [23] are available for Si_2CH_8, and Si_2C is a JANAF listed species. Thus, once again, unknown Si_2CH_x species parameters can be estimated by following the patterns seen in Si_3H_x and C_3H_x family tables. A few other heats of formation for carbon–silicon species have been measured or estimated. These include values for SiC_2H_4 [24], SiC_2H_6 [25], SiC_2H_8 [12], and both Si_2C_2 and Si_2C_3 [26]. Also, with SiH_3CH_3 [12] and SiC [11] being well known, it is possible to fill in estimates for a number of $SiCH_x$ species. However, none of these latter silicon–carbon species are important in the model even after allowing for the uncertainties in their thermodynamic parameters.

On the other hand, Si_2C is predicted to be important, and use of a recent ab initio calculation of its structure [27] and new matrix vibrational frequencies [28] to construct a different thermodynamic model would result in predictions of about twice as much Si_2C at high temperatures compared to the JANAF model used here with no change in the assumed heat of formation. Clearly, uncertainties of this magnitude exist for many of the species considered here, but our conclusions are unaffected by factor of two changes in predicted species concentrations.

2.3. Chemical kinetic data base

The reaction rate data base divides naturally into two areas: one for propane decomposition which includes carbon species only and one which includes both silicon and organosilicon species since they are often studied together. The propane decomposition reactions are taken from the pyrolysis modeling study of Edelson and Allara [29]. They performed a sensitivity analysis for their mechanism, and we used all of their reactions that received high ratings. Additional reactions which are more important in a dilute mixture of C_3H_8 in H_2 than in the pure C_3H_8 system considered in ref. [29] were also included.

A basic set of silane decomposition chemical kinetics was provided by the modeling study of Coltrin, Kee, and Miller [30]. We incorporated this set into our calculations. We did an analysis of the original experiments [31] on the initial decomposition step of SiH_4 going to SiH_2 and H_2 to provide a rate expression which was better adapted to our conditions. At high temperatures, the result from this fit was slightly faster than the

expression of Coltrin et al., so we continued to use their simpler form. Beyond this reaction set, there are only a few measured or estimated reaction rates for species in the deposition system, but they covered the important types of reactions and allowed estimates for all needed reactions to be made by analogy. These reactions include SiH_2 insertion into Si_2H_6 (originally studied by Bowrey and Purnell [32]), SiH_2 insertion into CH_4 and H_2 elimination from the SiH_3CH_3 which is formed [33], and SiH_2 insertion into SiH_3CH_3 [20]. Recent work [34,35] which showed very fast SiH_2 insertion into a number of substrates appeared after this study was completed, but these data would not affect the conclusions reported here.

3. Results of the calculations

3.1. Equilibrium concentrations

The results of equilibrium calculation are summarized in figs. 2 through 4 which show plots of silicon, carbon, and silicon-carbon species concentrations as functions of temperature. The first observation which can be made is that essentially all the propane should decompose, and most of it should form methane which is favored by the large excess of hydrogen carrier gas. The next non-silicon containing carbon species, acetylene, has an equilibrium concentration almost two orders of magnitude lower at the growth temperature (1673 K) and substantially less than this at ramp temperatures. At the growth temperature, the methyl radical concentration is an order of magnitude below that of acetylene, and ethylene is down another factor of two. The major equilibrium product of silane decomposition is SiH_2, although a significant amount of SiH_4 remains. The only other species having concentrations within an order of magnitude of SiH_2 are SiH, Si atoms, and Si_3. Down another order of magnitude are the Si_2H_x species Si_2H, Si_2, and either Si_2H_3 or Si_2H_2 depending on the thermodynamic parameter set involved. Finally, of the species having silicon–carbon bonds, only Si_2C and SiH_3CH_3 are potentially important. In equilibrium, Si_2C is predicted to be a major species

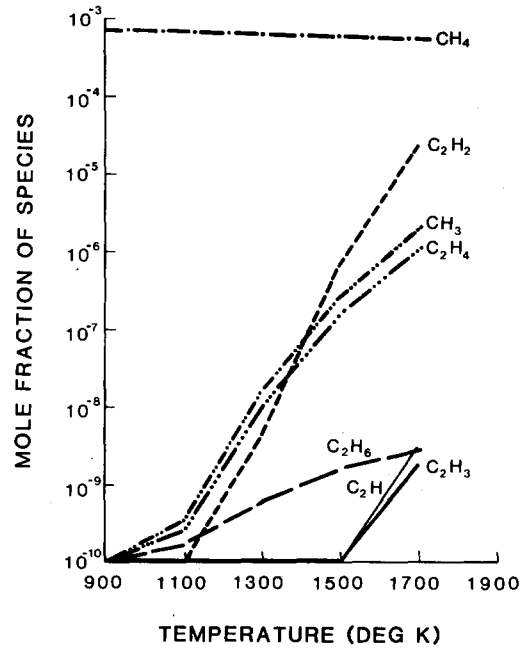

Fig. 2. Equilibrium carbon species.

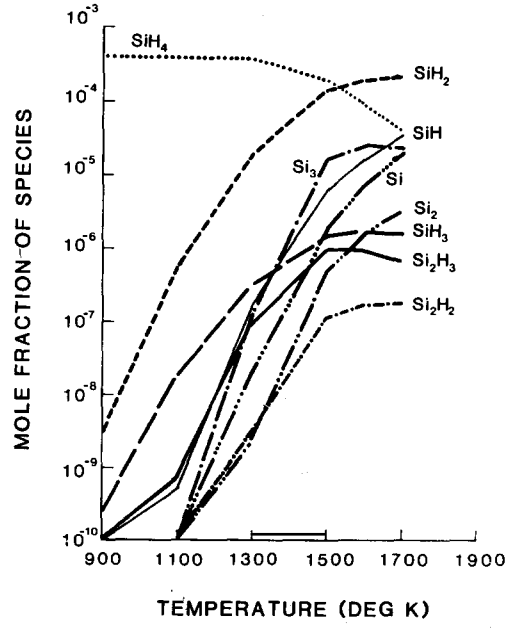

Fig. 3. Equilibrium silicon species.

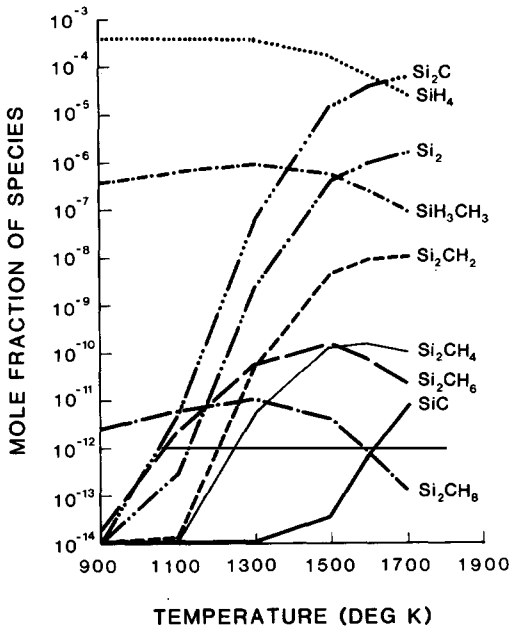

Fig. 4. Equilibrium silicon–carbon species.

containing almost as much silicon as does SiH_2. SiH_3CH_3 is a minor species, but one of the best candidates, along with Si_2, to be an important intermediate on the way to Si_2C formation. In summary, there are only a few important species, and most of them have quite well characterized thermochemistry.

3.2. Kinetically controlled concentrations

In evaluating various chemical kinetic mechanisms, well over 50 elementary reactions were used at one time or another. These reactions, their rate constants, and appropriate references are summarized in tables 2 and 3 found in appendix A. Many of these reactions are only minor contributors, and this set can be reduced without producing any significant changes in the predictions. Fig. 5 is a diagram of the pathways included in one such reduced set. This will serve to focus the discussion of which species may not reach equi-

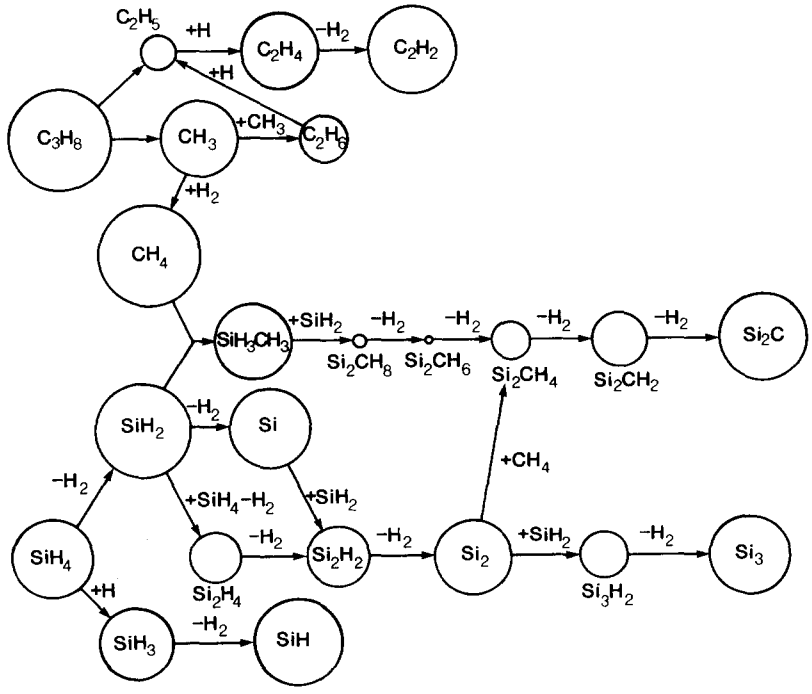

Fig. 5. Major pathways in the modeling of silicon carbide chemical vapor deposition. For SiH_4 and C_3H_8, the diameter of the circle is proportional to the log of their initial concentration. For the remaining species, the circle diameter is proportional to the log of their equilibrium concentration at 1673 K.

librium levels. The reactions included in this reduced set are summarized in table 4.

Beginning at the top of the diagram in fig. 5, C_3H_8 decomposition proceeds by an initial splitting into CH_3 and C_2H_5 radicals. The C_2H_5 can lose hydrogen to produce the stable molecules C_2H_4 and C_2H_2, but C_2H_6 is primarily formed by CH_3 recombination. It is through CH_3 abstraction of a hydrogen atom from H_2 that most of the CH_4 must be formed. This relatively slow reaction turns out to be one of the potential kinetic bottlenecks. As a result, more CH_3 and less CH_4 are predicted kinetically than are predicted by the equilibrium calculations.

The overabundance of CH_3 leads to larger C_2H_6 concentrations. In turn, hydrogen atoms can abstract a hydrogen to return C_2H_6 to C_2H_5, which is seen to be connected to C_2H_4 and C_2H_2. Naturally, all reactions indicated can proceed in both directions, and when C_2H_5 is initially in excess, it is a source. At all times the kinetic predictions for all C_2H_x species are larger than the equilibrium levels.

The kinetic analysis of C_3H_8 decomposition summarized in fig. 5 was obtained by comparing the equilibrium carbon species concentrations as plotted in fig. 2 with the results of an example kinetic calculation shown in fig. 6. In fig. 6, the abscissa represents distance above the substrate surface. For simplicity, only data for distances within 10^{-3} m above the surface are shown. In proceeding along a path normal to the surface over this distance, the temperature rises from 1610 K in the gas to 1665 K at the surface. The complete reaction sequence used in these calculations is given in table 2. It can be seen that conversion of CH_3 to CH_4 is not complete at the substrate surface and as a result the concentrations of C_2H_2, C_2H_4, C_2H_5, and C_2H_6 are all higher than their equilibrium values.

The complete set of reactions used to describe SiH_4 decomposition is given in table 3. Kinetic calculations of the decomposition products near the substrate are shown in fig. 7 for a substrate temperature of 1665 K. Comparing fig. 7 with fig. 3, the corresponding equilibrium result, we can see that all silicon species concentrations agree to well within an order of magnitude between the equi-

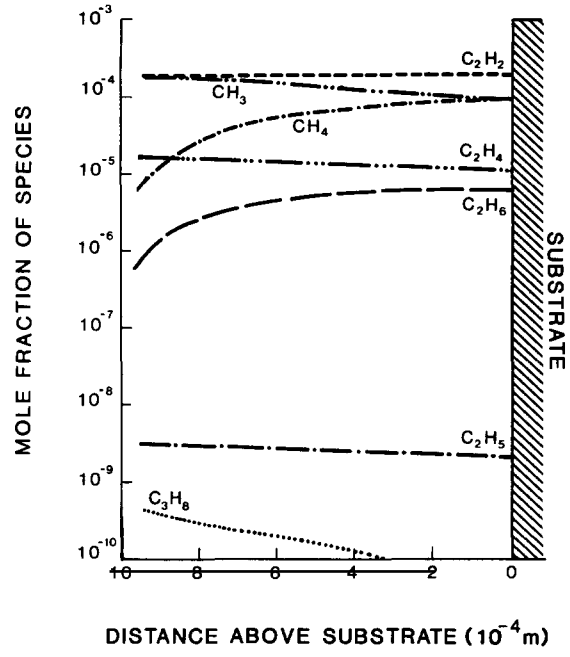

Fig. 6. Kinetically limited carbon species for a 1665 K substrate temperature.

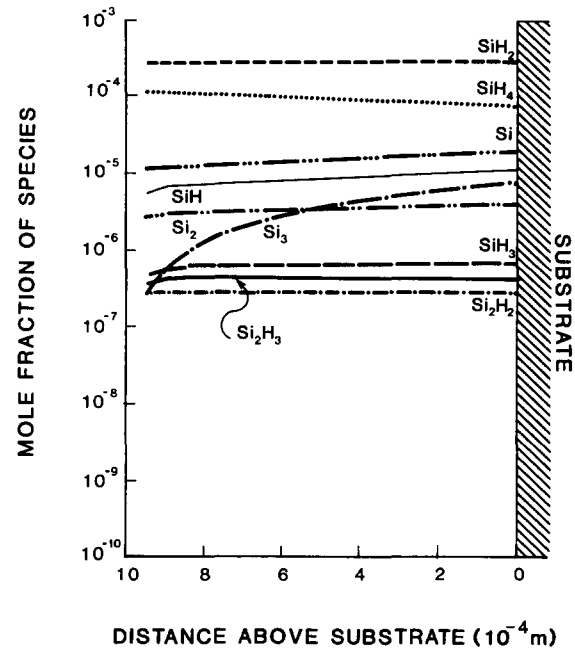

Fig. 7. Kinetically limited silicon species for a 1665 K substrate temperature.

librium and kinetic calculations over the last segment of a fast-changing temperature profile. As illustrated in fig. 5, the major pathway for SiH_4 decomposition is into SiH_2 and H_2. The minor branch to SiH_3 is adequate to maintain essentially equilibrium values of this radical. Formation of all the other important silicon species proceeds by H_2 elimination and SiH_2 insertion steps, all of which are fast enough that concentrations are kept quite close to equilibrium values as the molecules approach the hot wall.

The formation of Si_2C through several kinetic mechanisms was investigated. We note that available experimental and theoretical evidence points to a symmetric structure (Si–C–Si) for Si_2C [15]. No reaction mechanism could be found which both favored this structure as an initial product and gave significant Si_2C production. Of course, rearrangement of an intermediate to give a more stable final product is possible. With this assumption, some reaction sets were found which at least produced non-negligible amounts with plausible rate constants, and the best two are shown in fig. 5.

The first Si_2C formation sequence is shown in table 5 and begins with the formation of SiH_3CH_3 by insertion of SiH_2 into CH_4. This is efficient enough that the kinetically controlled SiH_3CH_3 concentration is indeed able to attain the equilibrium level (SiH_3CH_3 is the next most populous species containing a silicon–carbon bond). Then, a second SiH_2 insertion leads to Si_2CH_8, followed by successive H_2 eliminations which eventually result in Si_2C. In this mechanism, both SiH_2 insertion reaction rates have a basis in kinetic observations, while the H_2 elimination rates may at least be expected to be similar to those for well-studied analogous reactions. The $SiH_2 + CH_4$ rate we used is still almost an order of magnitude lower at high temperatures than the room temperature value recently reported by Inoue and Suzuki [34]. However, it is not slow formation of SiH_3CH_3, but rather its low equilibrium concentration, which limits this mechanism. The complete reaction sequence used in kinetic calculations for this mechanism is given in tables 4 and 5, and results for a substrate temperature of 1665 K are shown in figure 8.

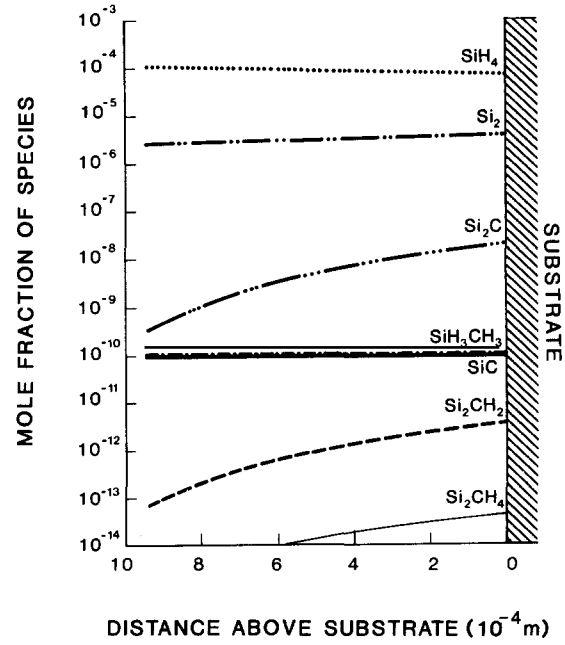

Fig. 8. Kinetically limited silicon–carbon species using the Si_3CH_3 decomposition mechanism for a 1665 K substrate temperature.

The second mechanism for Si_2C formation is shown in table 6 beginning with a reaction which has not been studied experimentally. The assumption was made that the Si_2 molecule is as reactive as SiH_x radicals and can insert into CH_4 with a similar rate. If this were true, then the Si_2CH_4 formed need only eliminate two hydrogen molecules to yield Si_2C. The complete reaction sequence used in kinetic calculations for this mechanism is given in tables 4 and 6, and results for a substrate temperature of 1665 K are shown in fig. 9.

For nominal rate constants, the Si_2C concentrations formed from each of these two parallel mechanisms are essentially equal, but they are more than three orders of magnitude below the equilibrium level. This is seen by comparing the equilibrium results in fig. 5 with the kinetically controlled concentrations for the two mechanisms as plotted in figs. 8 and 9. It is seen that the two-atom precursors SiH_3CH_3 and Si_2 reach essentially their equilibrium values (in fact Si_2 exceeds it because difficulties in forming larger sili-

con species push more silicon into the remaining molecules). These concentrations are not large however, and this makes formation of Si_2C unlikely.

A number of other mechanisms were investigated, both for Si_2C formation and for the potentially analogous case of Si_3 formation. In the latter case, formation of Si_2, insertion of SiH_2, and loss of H_2 from Si_3H_2 is an adequate pathway. An analog of this mechanism for Si_2C is not useful due to the instability of SiC on the one hand and the small concentration of CH_2 on the other. Thus, based on these results we can only conclude that there is a good chance that Si_2C and other gaseous species with silicon–carbon bonds are in fact not formed in silicon carbide deposition systems.

By performing similar kinetic calculations for different substrate temperatures, it is possible to identify the key gas phase species which must react on the surface at specific temperatures during the initial and crystal growth phases. The results of these calculations are summarized in table 1. It should be noted that the silicon and carbon species are listed in order of decreasing concentration, and species below the 10^{-6} level are not listed since is is unlikely that they contribute significantly to the deposition process.

Table 1
Key deposition species

Gas species	Temperature range (K)	Growth regime
SiH_4, C_3H_8	$T < 1050$	Initial
SiH_4, C_2H_4, CH_3, CH_4	$1050 < T < 1300$	Initial
SiH_2, SiH_4, C_2H_2, CH_4, C_2H_4	$1300 < T < 1673$	Initial/crystal

Comparing the results summarized in table 1 with the equilibrium calculations shown in figs. 2 and 3, it is evident that kinetics alters both the identity and relative concentration of the hydrocarbon species which react on the surface to form SiC. Moreover, different species can be associated with specific temperature ranges and growth regimes. More to the point, there is clearly a difference in the identity of the reactive species in the initial and crystal growth regimes as well as within the initial growth regime.

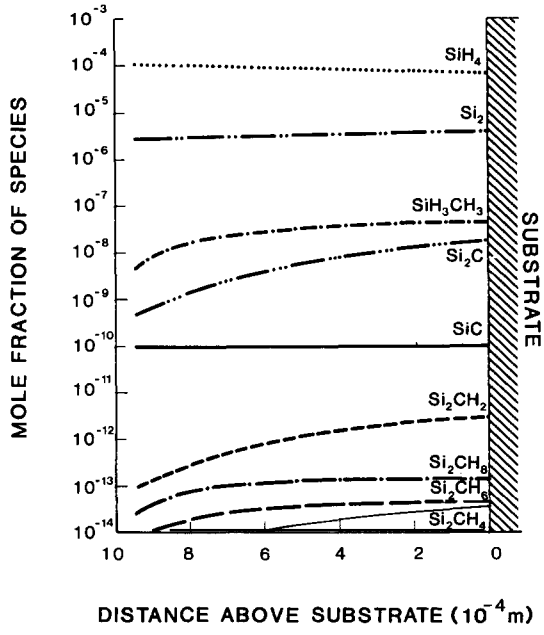

Fig. 9. Kinetically limited silicon–carbon species using the $Si_2 + CH_4$ mechanism for a 1665 K substrate temperature.

4. Discussion and conclusions

In assessing the results of these calculations, several points concerning the gas phase chemistry can be made. The SiH_4 decomposition products are seen to be near equilibrium levels for essentially all deposition conditions. In contrast, the C_3H_8 decomposition products have difficulty in attaining their equilibrium levels, although significant decomposition is achieved at lower temperatures than for silane. At low temperature (< 1050 K) in the initial growth regime, C_3H_8 rather than CH_4, the equilibrium species, is the primary carbon containing species which must interact with the surface. At intermediate temperatures (1050 to 1300 K) in the initial growth regime, C_3H_8 decomposition occurs, but C_2H_4 and CH_3 are present at higher levels than CH_4. Only at the highest temperatures (1300 to 1673 K) in the initial growth

and crystal growth regimes does CH_4 approach its equilibrium level, and even at these temperatures, the C_2H_2 and C_2H_4 levels are higher than at equilibrium.

The questions which must now be addressed concern the implications of these results on our understanding of the two step β-SiC deposition process. Does the multiplicity of hydrocarbon species produced by gas phase kinetic limitations cause any inherent differences between initial and crystal growth mechanisms? Additionally, does this result have implications with respect to the need for and role of the initial growth step?

The answer to these questions is yes only if the surface reactivity of the C_3H_8 decomposition products like C_2H_4 and C_2H_2 differs from that of CH_4 which dominates the deposition species under equilibrium conditions. Fischman and Petuskey [36] have previously suggested that differences in the surface reactivity or reactive sticking coefficients could play a role in the SiC deposition process. Intuitively, we expect molecules like C_2H_4 and CH_4 to have different sticking coefficients. At low temperatures, this has been confirmed by the work of Yates and co-workers [37] and Ceyer and co-workers [38]. Studies in our laboratory indicate that this is also true for temperatures relevant to SiC deposition [39].

With this added insight we propose the following hypothesis. During the initial growth regime, gas phase kinetics provide reactive C_3H_8 decomposition products to the Si surface. These reactive hydrocarbons initiate SiC deposition at relatively low temperatures. Because of the propensity toward surface nucleation at low temperatures, the resulting thin films have a large number of grain boundaries which can accommodate the Si–SiC lattice mismatch. These grain boundaries also allow rapid out-diffusion of Si needed to form the initial SiC deposit. Because the initial film growth is carried out mainly at higher temperatures, the surface mobility of the carbon (and silicon) atoms is sufficient to allow epitaxial ordering of the individual grains relative to the substrate. This would be consistent with Addamiano's [7] observations that the initial layers were single crystal but strained with a large number of internal surfaces. This model is also consistent with the observation that CVD of "good" SiC is accompanied by the formation of a large number of pits in the Si substrate.

The rationale for a ramp during initial growth, then, could be the need for hydrocarbon species with high sticking coefficients at low temperatures, coupled with the need for higher temperatures to give high surface mobilities. The insensitivity of the initial growth phase to the presence of SiH_4 could be accounted for by the fact that SiH_4 remains essentially undissociated during much of the initial deposition and that the hydrocarbon species probably react more rapidly than SiH_4. The Si required to form SiC during this stage of the deposition process is available from the substrate.

The oriented microcrystals of SiC formed during the initial growth period provide the substrate for SiC homoepitaxy during the crystal growth period. At the temperatures encountered during crystal growth, SiH_4 decomposes largely to the more reactive SiH_2 radical species. These react with the available impinging hydrocarbon species on the evolving SiC surface. It should be noted that the transport of either Si or C through the SiC deposit is precluded by the low diffusivity of these species in SiC, and, presumably, grain boundary diffusion is no longer a factor once epitaxial growth begins [40,41]. The formation of such a diffusion barrier has been observed in related surface studies by Yates and co-workers [37].

For deposits grown by first exposing the surface at high temperature to the hydrocarbon reactant (i.e., without a ramp), the low nucleation probability leads to a small number of grains. This most likely produces extended defects as the grains grow to cover the surface. Initiating growth at high temperature with a SiH_4 and C_3H_8 mixture also raises the possibility that Si growth from SiH_2 or other reactive species will compete with SiC growth. Thus, the quality and reproducibility of SiC grown without the initial temperature ramp would be quite limited.

In summary, potential differences in surface reaction rates may result in a sensitivity to the gas phase kinetics and therefore to deposition conditions such as gas composition, flow rate, and

substrate temperature and its uniformity. The impact of these differences in surface chemistry may be quite extensive. Differences in species reactivity may lead to deposits which transmit orientation information and accommodate the lattice mismatch. Whatever the actual situation, however, it is evident that information on the surface chemistry of individual carbon containing species is required to develop an understanding of the two step deposition mechanisms for β-SiC. We are presently involved in studies to resolve these and other issues related to the surface chemistry of SiC deposition.

Acknowledgements

This work was supported by the National Aeronautics and Space Administration under contract number NAS 3-24531. We wish to thank M.A. Kuczmarski, J.A. Powell, L.G. Matus, and G.T. Seng of the NASA Lewis Research Center and Professor P.P. Gaspar of Washington University, St. Louis, for many helpful discussions throughout the course of this work.

Table 2
Reaction list for C_3H_8 decomposition

Reaction	A	E (kcal/mol)
$C_3H_8 \rightarrow CH_3 + C_2H_5$	7.94E16	85.1
$C_3H_8 + H \rightarrow C_3H_7 + H_2$	2.10E-13	9.7
$C_3H_8 + CH_3 \rightarrow C_3H_7 + CH_4$	1.67E-15	11.5
$C_3H_8 + C_2H_5 \rightarrow C_3H_7 + C_2H_6$	5.27E-16	12.3
$C_3H_7 \rightarrow H + C_3H_6$	1.58E13	38.6
$C_3H_6 + H \rightarrow C_3H_5 + H_2$	1.67E-13	3.5
$C_3H_8 + C_3H_5 \rightarrow C_3H_7 + C_3H_6$	1.32E-15	20.5
$C_3H_6 + CH_3 \rightarrow C_3H_5 + CH_4$	2.64E-16	8.8
$C_3H_5 + H_2 \rightarrow C_3H_6 + H$	5.27E-14	19.7
$C_3H_7 \rightarrow CH_3 + C_2H_4$	1.26E13	32.5
$C_2H_4 + H \rightarrow C_2H_5$	6.64E-14	2.6
$CH_3 + CH_3 \rightarrow C_2H_6$	4.19E-14	0.0
$CH_3 + H_2 \rightarrow H + CH_4$	2.64E-15	11.3
$C_2H_5 + H_2 \rightarrow C_2H_6 + H$	6.64E-15	14.0
$C_3H_8 + 2\text{-}C_3H_7 \rightarrow 1\text{-}C_3H_7N + C_3H_8$	1.70E-16	12.9
$C_3H_7 + C_3H_7 \rightarrow C_3H_6 + C_3H_8$	1.70E-14	0.0
$C_3H_7 + CH_3 \rightarrow C_3H_6 + CH_4$	4.20E-15	0.0
$C_3H_5 + C_3H_7 \rightarrow C_3H_6 + C_3H_6$	1.70E-15	0.0

All rate constant parameters in the above table were taken from Edelson and Allara [29]. In addition, a rate coefficient for $C_2H_2 + H_2 \rightarrow C_2H_4$ of $7.6 \times 10^{-12}\ T \exp(-36.52/RT)$ taken from Westbrook and Dryer [44] was included.

Appendix A: Model reaction mechanisms

The tables 2–6 list the model reaction mechanisms used in this study. The parameters A and E

Table 3
Reaction list for SiH_4 decomposition

Reaction	A	E (kcal/mol)
$SiH_4 \rightarrow SiH_2 + H_2$	5.00E12	52.2
$SiH_4 + Si \rightarrow SiH_2 + SiH_2$	1.55E-11	2.0
$Si + H_2 \rightarrow SiH_2$	1.92E-10	2.0
$SiH_2 + Si \rightarrow Si_2H_2$	1.21E-11	2.0
$Si_2 + H_2 \rightarrow Si_2H_2$	2.57E-11	2.0
$Si + Si_3 \rightarrow Si_2 + Si_2$	3.43E-12	24.1
$SiH_2 + Si_3 \rightarrow Si_2H_2 + Si_2$	2.38E-13	18.8
$SiH_3SiH + H_2 \rightarrow SiH_4 + SiH_2$	1.04E-7	2.0
$Si_2H_4 + H_2 \rightarrow SiH_4 + SiH_2$	1.04E-7	2.0
$Si_2H_2 + H_2 \rightarrow SiH_3SiH$	4.08E-10	2.0
$Si_2H_2 + H_2 \rightarrow Si_2H_4$	4.08E-10	2.0
$SiH_4 + SiH_4 + SiH_2 \rightarrow Si_2H_6$	8.35E-12	1.29
$SiH_4 + SiH_3 \rightarrow Si_2H_5 + H_2$	2.95E-12	4.4
$SiH_4 + SiH \rightarrow SiH_3 + SiH_2$	2.30E-12	11.2
$SiH_4 + SiH \rightarrow Si_2H_5$	4.88E-12	2.0
$SiH_2 + SiH \rightarrow Si_2H_3$	2.10E-11	2.0
$SiH + H_2 \rightarrow SiH_3$	5.75E-11	2.0
$Si_2H_3 + H_2 \rightarrow Si_2H_5$	4.93E-11	2.0
$SiH_4 \rightarrow SiH_3 + H$	3.69E15	93.0
$SiH_4 + H \rightarrow SiH_3 + H_2$	1.73E-10	2.5
$SiH_3SiH + H_2 \rightarrow Si_2H_6$	1.55E-11	2.0
$Si_2H_4 + H_2 \rightarrow Si_2H_6$	1.55E-11	2.0
$Si_2H_2 + H \rightarrow Si_2H_3$	1.44E-9	2.0
$Si_2H_6 + SiH_2 \rightarrow Si_3H_8$	1.10E-12	0.4
$Si_3H_8 \rightarrow Si_3H_6 + H_2$	2.50E14	48.9
$Si_3H_6 \rightarrow Si_3H_4 + H_2$	2.50E14	44.4
$Si_3H_4 \rightarrow Si_3H_2 + H_2$	2.50E14	32.4
$Si_3H_2 \rightarrow Si_3 + H_2$	2.50E14	23.7
$Si_2 + SiH_4 \rightarrow Si_3H_4$	1.00E-12	0.0
$Si_2 + SiH_2 \rightarrow Si_3H_2$	1.00E-12	0.0
$Si_2H_3 + SiH_4 \rightarrow Si_3H_7$	1.00E-12	0.0
$Si_2H_3 + SiH_2 \rightarrow Si_3H_5$	1.00E-12	0.0
$Si_2H_2 + SiH_4 \rightarrow Si_3H_6$	1.00E-12	0.0
$Si_3H_7 + H \rightarrow Si_3H_8$	1.00E-12	0.0
$Si_2H_2 + SiH_2 \rightarrow Si_3H_4$	1.00E-9	0.0
$Si_3H_5 + H \rightarrow Si_3H_6$	1.00E-9	0.0

The parameters for the first 23 reactions are taken from Coltrin, Kee, and Miller [30]; those for $Si_2H_6 + SiH_2$ are from White et al. [42], while the remaining values are estimates.

Table 4
Reduced reaction list for combined SiH_4 and C_3H_8 decomposition

Reaction	A	E (kcal/mol)
$SiH_4 \rightarrow SiH_2 + H_2$	5.00E12	52.2
$Si + H_2 \rightarrow SiH_2$	1.92E-10	2.0
$SiH_2 + Si \rightarrow Si_2H_2$	1.21E-11	2.0
$Si_2 + H_2 \rightarrow Si_2H_2$	2.57E-11	2.0
$SiH_2 + SiH \rightarrow Si_2H_3$	2.10E-11	2.0
$SiH + H_2 \rightarrow SiH_3$	5.75E-11	2.0
$SiH_4 \rightarrow SiH_3 + H$	3.69E15	93.0
$Si_3H_2 \rightarrow Si_3 + H_2$	2.50E14	23.7
$Si_2 + SiH_2 \rightarrow Si_3H_2$	1.00E-12	0.0
$C_3H_8 \rightarrow CH_3 + C_2H_5$	7.94E16	85.1
$C_2H_4 + H \rightarrow C_2H_5$	6.64E-14	2.6
$CH_3 + CH_3 \rightarrow C_2H_6$	4.19E-14	0.0
$CH_3 + H_2 \rightarrow H + CH_4$	2.64E-15	11.3
$C_2H_2 + H_2 \rightarrow C_2H_4$	7.62E-12	36.5

Table 5
Si_2H_8 mechanism for Si_2C formation

Reaction	A	E (kcal/mol)
$SiH_2 + CH_4 \rightarrow SiH_3CH_3$	5.00E-11	19.0
$SiH_2 + SiH_3CH_3 \rightarrow Si_2CH_8$	6.75E-12	0.4
$Si_2CH_8 \rightarrow Si_2CH_6 + H_2$	2.50E14	48.9
$Si_2CH_6 \rightarrow Si_2CH_4 + H_2$	2.50E14	44.4
$Si_2CH_4 \rightarrow Si_2CH_2 + H_2$	2.50E14	32.4
$Si_2CH_2 \rightarrow Si_2C + H_2$	2.50E14	23.7

The activation energy for the first reaction is taken from ref. [33], while the A factor is that for $SiH_2 + SiH_4$ reported by John and Purnell [43]. The parameters for the second reaction are taken from ref. [20], while the rest are estimates.

Table 6
Si_2 mechanism for Si_2C formation

Reaction	A	E (kcal/mol)
$Si_2 + CH_4 \rightarrow Si_2CH_4$	5.00E-9	19.9
$Si_2CH_4 \rightarrow Si_2CH_2 + H_2$	2.50E14	32.4
$Si_2CH_2 \rightarrow Si_2C + H_2$	2.50E14	23.7

determine the rate coefficient through $k = A \exp(-E/RT)$. The units of A depend on the reaction order but are given in terms of molecules, cubic centimeters, and seconds. Also note that $5.00E12 \equiv 5 \times 10^{12}$. Tables 2 and 3 show the complete reaction sequences used to describe C_3H_8 and SiH_4 decomposition, respectively. Based on a sensitivity analysis, the combined set of 56 elementary reactions shown in tables 2 and 3 was reduced to 14 reactions which were sufficient to accurately describe the behavior of key Si, C, and Si–C species. This reduced reaction sequence is shown in table 4. Tables 5 and 6 show the reactions leading to Si_2C via the Si_2CH_8 and Si_2 mechanisms, respectively. In the calculations, these reactions were added to the set shown in table 4.

References

[1] S. Nishino, Y. Hazuki, H. Matsunami and T. Tanaka, J. Electrochem. Soc. 127 (1980) 2674.
[2] H. Matsunami, S. Nishino and T. Tanaka, J. Crystal Growth 45 (1974) 138.
[3] D.K. Ferry, Phys. Rev. B12 (1975) 2361.
[4] S. Nishino, H. Suhara, H. Ono and H. Matsanami, J. Appl. Phys. 61 (1987) 4889.
[5] S. Nishino, J.A. Powell and H.A. Will, Appl. Phys. Letters 42 (1983) 460.
[6] P. Liaw and R.F. Davis, J. Electrochem. Soc. 132 (1985) 642.
[7] A. Addamiano and J.A. Sprague, Appl. Phys. Letters 44 (1984) 525.
[8] J.A. Powell, private communication, 1985.
[9] W.M. Kays, Convective Heat and Mass Transfer (McGraw-Hill, New York, 1966).
[10] C.D. Stinespring and J.C. Wormhoudt, Optimization of Silicon Carbide Production, ARI-RR-485 (Aerodyne Research, Inc., Billerica, MA, 1985).
[11] M.W. Chase et al., JANAF Thermochemical Tables Dow Chemical Co., Midland MI, updated periodically.
[12] S.W. Benson, Thermochemical Kinetics (Wiley, New York, 1976).
[13] D.R. Stull, E.F. Westrum and G.C. Sinke, The Thermodynamics of Organic Compounds (Wiley, New York, 1969).
[14] R. Walsh, Acc. Chem. Res. 14 (1981) 246.
[15] L. Fredin, R.H. Hauge, Z.H. Kafafi and J.L. Margrave, J. Chem. Phys. 82 (1982) 3542.
[16] C.D. Eley, M.C.A. Rowe and R. Walsh, Chem. Phys. Letters 126 (1986) 153.
[17] S.K. Shin and J.L. Beauchamp, J. Phys. Chem. 90 (1986) 1507.
[18] P. Ho, M.E. Coltrin, J.S. Binkley and C.F. Melius, J. Phys. Chem. 89 (1985) 4647.
[19] P. Ho, M.E. Coltrin, J.S. Binkley and C.F. Melius, J. Phys. Chem. 90 (1986) 3399.
[20] A.J. Vanderwielen, M.A. Ring and H.E. O'Neal, J. Am. Chem. Soc. 97 (1978) 993.
[21] K. Krogh-Jespersen, Chem. Phys. Letters 93 (1982) 327.
[22] J.P.M. Schmitt, P. Gressier, M. Krishnan, G. DeRosny and J. Perrin, Chem. Phys. 84 (1984) 281.

[23] H.E. O'Neal and M.A. Ring, J. Organometallic Chem. 213 (1981) 419.
[24] M.S. Gordon and R.D. Koob, J. Am. Chem. Soc. 103 (1981) 2939.
[25] D.D. Wagman, W.H. Evans, V.B. Parker, R.H. Schumm, I. Halow, S.M. Bailey, K.L. Churney and R.L. Nuttall, J. Phys. Chem. Ref. Data 11 (1982) 2.
[26] J. Drowart, G. DeMaria and M.G. Ingraham, J. Chem. Phys. 29 (1958) 1015.
[27] G.H.F. Diercksen, N.E. Gruner, J. Oddershede and J.R. Sabin, Chem. Phys. Letters 117 (1985) 29.
[28] Z.H. Kafafi, R.H. Hauge, L. Fredin and J.L. Margrave, J. Phys. Chem. 87 (1983) 797.
[29] D. Edelson and D. Allara, Intern. J. Chem. Kinetics 12 (1980) 605.
[30] M.E. Coltrin, R.J. Kee and J.A. Miller, J. Electrochem. Soc. 131 (1984) 425.
[31] C.G. Newman, H.E. O'Neal, M.A. Ring, F. Leska and N. Shipley, Intern. J. Chem. Kinetics 11 (1979) 1167.
[32] M. Bowrey and J.H. Purnell, Proc. Roy. Soc. (London) A321 (1971) 341.
[33] B.A. Sawrey, H.E. O'Neal, M.A. Ring and D. Coffey, Intern. J. Chem. Kinetics 16 (1984) 31.
[34] G. Inoue and M. Suzuki, Chem. Phys. Letters 122 (1985) 361.
[35] J.M. Jasinski, J. Phys. Chem. 90 (1986) 555.
[36] G.S. Fischman and W.T. Petuskey, J. Am. Ceram. Soc. 68 (1985) 185.
[37] F. Bozso, J.T. Yates, W.J. Choyke and L. Muehlhoff, J. Appl. Phys. 57 (1985) 2771.
[38] M.B. Lee, Q.Y. Yang, S.L. Tang and S.T. Ceyer, J. Chem. Phys. 85 (1986) 1693.
[39] C.D. Stinespring, X-Ray Photoelectron Spectroscopy Studies of Silicon Carbide Deposition: Initial Layer Growth (manuscript in preparation), and Report No. RP-236 (Aerodyne Research, Inc., Billerica, MA, 1986).
[40] R.C. Newman and J. Wakefield, J. Phys. Chem. Solids 19 (1961) 230.
[41] J.D. Hong, R.F. Davis and D.E. Newbury, J. Mater. Sci. 16 (1981) 2485.
[42] R.T. White, R.L. Espino-Rios, D.S. Rogers, M.A. Ring and H.E. O'Neal, Intern. J. Chem. Kinetics 17 (1985) 1029.
[43] P. John and J.H. Purnell, J. Chem. Soc. Faraday Trans. 69 (1973) 1485.
[44] C.K. Westbrook and F.L. Dryer, Progr. Energy Combust. Sci. 10 (1984) 1.